A Novel Piece-Wise Constant Analog Spiking Neuron Model and its Neuron-like Excitabilities

Yutaro Yamashita and Hiroyuki Torikai

***Abstract*— A novel analog spiking neuron model which has a *piece-wise constant* (ab. PWC) vector field and can be implemented by a simple electronic circuit is proposed. Using theories on discontinuous ODEs, the dynamics of the proposed model can be reduced into a one-dimensional return map analytically. Using the return map, it is shown that the proposed model can exhibit various neuron-like behaviors and bifurcations. It is also shown that the model can reproduce not only the individual neuron-like behaviors and bifurcations but also relations among them that are typically observed in biological and model neurons.**

***Index Terms*— Spiking neuron model, Bifurcation, Excitability, Electronic hardware neuron**

I. Introduction

SPIKING neuron models and their electronic hardware implementations have been studied intensively, where many models are described by nonlinear *ordinary differential equations* (ab. ODEs) like Hodgkin-Huxlay model or nonlinear ODEs with state-dependent resets like Izhikevich model [1]-[8]. Neurons exhibit various behaviors such as resting state, subthreshold oscillation, spiking state and bursting state (that are called *neural behaviors* in this paper) depending on stimulation inputs and parameter values. Also, neurons exhibit various nonlinear phenomena such as local and global bifurcations. It is known that neural behaviors and bifurcations of neurons often have closed relations, where typical ones are summarized in Table I [9]. So, one of the fundamental problems in a research of artificial spiking neuron modeling is to reproduce such relations. In this paper we propose a novel *piece-wise constant* (ab. PWC) analog spiking neuron model which can be implemented by a simple electronic circuit. The dynamics of the proposed model is described by an ODE with PWC characteristics together with a state-dependent reset. Using theories on discontinuous ODEs [10], the dynamics of the proposed model can be reduced into a one-dimensional return map analytically. Using the return map, it is shown that the proposed model can exhibit various neural behaviors and related bifurcations. It is also shown that the model can reproduce three out of four relations among neural behaviors and bifurcations in Table I (i.e., supercritical Hopf, saddle-node off invariant circle, and saddle-node on invariant circle type bifurcations) that are typically observed in biological and model neurons. Furthermore, it is shown that the other bifurcation (i.e., subcritical Hopf type bifurcation) cannot be directly reproduced but its accompanying bifurcation can be reproduced. Significances and novelties of this paper include the following points. **(1)** This paper proposes an analog spiking neuron model having a PWC vector field for the first time. Advantages of the PWC vector field include: easy to implement by a simple electronic circuit, easy to tune parameter values, and suitability for theoretical analysis based on theories on discontinuous ODEs [10] (compared to implementation methods of nonlinear ODE models [2]-[8]). **(2)** The neural prosthesis is a recent hot topic, where a typical approach is to prosthesize a damaged part of neural systems by a digital processor [11], [12]. On the other hand, sensory neurons should be prosthesized by analog electronic circuits since sensory neurons accept analog signals and it is not so efficient to utilize digital processor neurons together with analog-to-digital converters to implement them. Due to the advantages in the previous point (1), the proposed model is suitable for a sensory neuron prosthesis as well as a hardware pulse-coupled neural network. **(3)** The proposed model can be regarded as a generalized version of a PWC oscillator in [13]-[15]. However, the oscillator is designed as an abstract chaotic oscillator and cannot exhibit neural behaviors.

TABLE I

Reproduction of typical relations among neural behaviors and bifurcations by PWC analog spiking neuron model.

Relations among neural behaviors and bifurcations [9]			Reproduction by PWC analog spiking neuron model
Subthreshold oscillation	Co-existence of resting and spiking states	Bifurcation	
Yes	No	Supercritical Hopf	Yes Scenario A in Eq.(5)
Yes	Yes	Subcritical Hopf	Partially Scenario B in Eq.(6)
No	Yes	Saddle-node off invariant circle	Yes Scenario C in Eq.(13)
No	No	Saddle-node on invariant circle	Yes Scenario D in Eq.(15)

II. Piecewise Constant Analog Spiking Neuron Model

A novel *piece-wise constant* (ab. PWC) analog spiking neuron model is presented in Fig.1(a). The model consists of two capacitors, two *operational transconductance amplifiers* (ab. OTAs), a comparator, a monostable multivibrator, an analog switch, an amplifier, an adder, and an absolute value circuit. Fig.1(b) shows the characteristics of the OTA: it outputs a positive (negative) current if the differential voltage $v_\varepsilon = v^+ - v^-$ is positive (negative). From a viewpoint of neuron model, the capacitor voltages v and u can be regarded as an membrane potential and a recovery variable, respectively, as explained in the table in Fig.1. Also, an input voltage V_{in} and a constant voltage V_T can be regarded as a stimulation input and a spiking threshold, respectively. The constant voltage V_T is also regarded as a spike cut-off level

978-1-4244-9637-2/11/$26.00 ©2011 IEEE

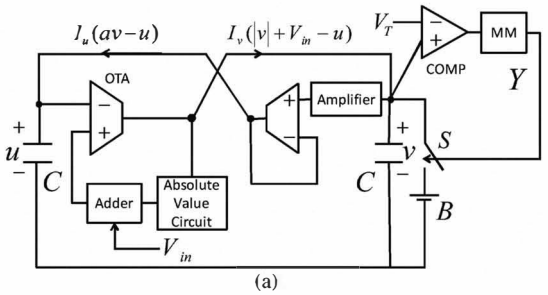

(a)

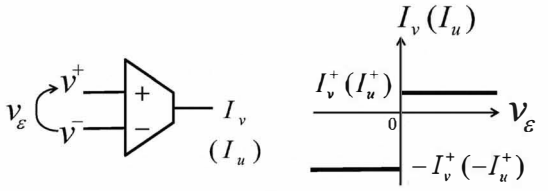

(b)

PWC spiking neuron	Meaning as a neuron model
Capacitor voltage v	Membrane potential
Capacitor voltage u	Recovery variable
Input voltage V_{in}	Stimulation input
Constant voltage V_T	Spiking threshold
Spike-train Y	Output firing spike-train

Fig. 1. PWC analog spiking neuron model. (a) Electrical circuit model. COMP and MM represent the monostable multivibrator and the comparator, respectively. (b) Characteristics of the *operational transconductance amplifier* (ab. OTA).

[9]. If the membrane potential v reaches the spiking threshold V_T, the comparator (COMP) triggers the monostable multivibrator (MM) to generate a spike $Y = E$. The spike $Y = E$ closes the analog switch S for a short time, and then the membrane potential v is reset to a constant value B which is called a reset base. From a viewpoint of neuron model, the spike $Y = E$ is regarded as a firing spike or an action potential as explained in the table in Fig.1. The dynamics of the PWC analog spiking neuron model is described by the following equation.

$$\begin{cases} C\dot{v} = I_v(|v| + V_{in} - u) \\ C\dot{u} = I_u(av - u) \end{cases} \quad \text{if } v < V_T,$$
$$v(t^+) = B \quad \text{if } v(t) = V_T,$$
$$I_v(v_\varepsilon) = \begin{cases} I_v^+ & \text{if } v_\varepsilon > 0 \\ -I_v^- & \text{if } v_\varepsilon < 0 \end{cases} \qquad (1)$$
$$I_u(v_\varepsilon) = \begin{cases} I_u^+ & \text{if } v_\varepsilon > 0 \\ -I_u^- & \text{if } v_\varepsilon < 0 \end{cases}$$
$$Y(t^+) = \begin{cases} E & \text{if } v(t) = V_T \\ -E & \text{if } v(t) < V_T \end{cases}$$

where "$\dot{}$" represents the time derivative, t^+ represents $\lim_{\varepsilon \to +0}(t+\varepsilon)$, I_v^+, I_v^-, I_u^+, $I_u^- > 0$ are assumed, and $v(0) \le V_T$ is assumed. In the whole state space

$$\boldsymbol{S} \equiv \{(v,u) | v \le V_T\},$$

the following two borders are defined by the control voltages of the two OTAs (see also Fig.2(a)):

$$v\text{-nullcline}: \quad \boldsymbol{N}_v \equiv \{(v,u) | u = |v| + V_{in}\},$$
$$u\text{-nullcline}: \quad \boldsymbol{N}_u \equiv \{(v,u) | u = av\},$$

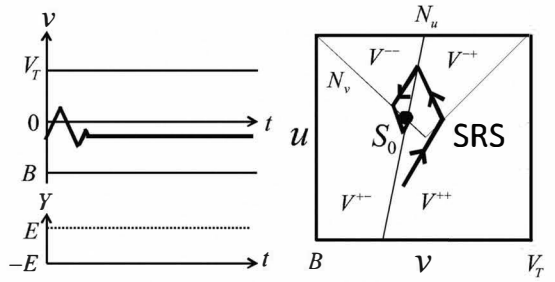

(a) *Stable resting State* (SRS).

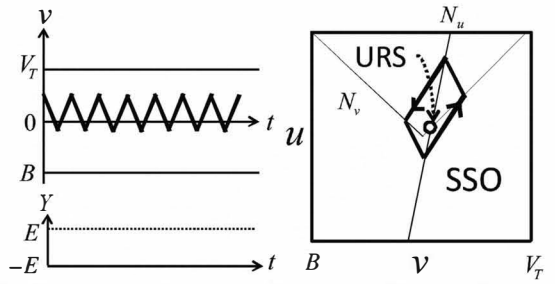

(b) Co-existence of *stable subthreshold oscillation* (SSO) and *unstable resting state* (URS).

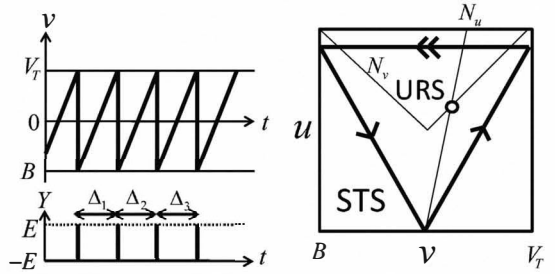

(c) Co-existence of *stable tonic spiking* (STS) and *unstable resting state* (URS).

Fig. 2. Basic behaviors of the PWC analog spiking neuron model.

where " $\equiv$ " represents the "definition" hereafter. Since the borders play the same roles as nullclines of a smooth nonlinear ODE, the borders are called v-nullcline and u-nullcline. The nullclines divide the whole state space $\boldsymbol{S}$ into at most four subspaces having the following four vector fields (see also Fig.2(a)):

$$(\dot{v}, \dot{u}) =$$
$$\begin{cases} \boldsymbol{V}^{++} \equiv (I_v^+/C, I_v^+/C) & \text{if } u < |v| + V_{in} \text{ and } u < av, \\ \boldsymbol{V}^{-+} \equiv (I_v^-/C, I_v^+/C) & \text{if } u > |v| + V_{in} \text{ and } u < av, \\ \boldsymbol{V}^{+-} \equiv (I_v^+/C, I_v^-/C) & \text{if } u < |v| + V_{in} \text{ and } u > av, \\ \boldsymbol{V}^{--} \equiv (I_v^-/C, I_v^-/C) & \text{if } u > |v| + V_{in} \text{ and } u > av. \end{cases}$$

According to [10], the dynamics of the state (v,u) on the nullclines $\boldsymbol{N}_v$ and $\boldsymbol{N}_u$ can be categorized into *sliding mode* and *non-sliding mode* (we also say "*without sliding mode*"). In the following Sections III and IV, neuron-like excitabilities of the PWC analog spiking neuron model without and with the sliding modes are studied, respectively.

III. Excitabilities without Sliding-mode

In this section we assume

$$1 < \frac{I_u^+}{I_v^+}, \frac{I_u^+}{I_v^-}, \frac{I_u^-}{I_v^-}, \frac{I_u^-}{I_v^+} < a. \qquad (2)$$

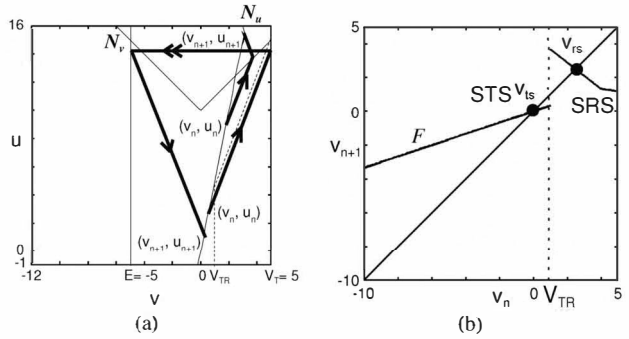

Fig. 3. Phase-plane trajectory and return map F.

In this case, according to [10], the nullclines $\boldsymbol{N}_v$ and $\boldsymbol{N}_u$ have no sliding mode dynamics. Then the dynamics of the state vector (v,u) on the nullclines $\boldsymbol{N}_v$ and $\boldsymbol{N}_u$ can be described by

$$(\dot{v},\dot{u}) = \begin{cases} \boldsymbol{V}^{++} & \text{if } (v,u) \in \boldsymbol{N}_u \text{ and } u < |v| + V_{in}, \\ \boldsymbol{V}^{+-} & \text{if } (v,u) \in \boldsymbol{N}_v \text{ and } u > av, \\ \boldsymbol{V}^{-+} & \text{if } (v,u) \in \boldsymbol{N}_v \text{ and } u < av, \\ \boldsymbol{V}^{--} & \text{if } (v,u) \in \boldsymbol{N}_u \text{ and } u > |v| + V_{in}, \\ (0,0) & \text{if } (v,u) \in \boldsymbol{N}_v \cap \boldsymbol{N}_u, \end{cases}$$

where the state vector (v,u) is continuous before and after crossing a nullcline. Fig.2 shows the following typical neuron-like behaviors of the PWC analog spiking neuron model.

Resting state. The intersection point $\boldsymbol{S}_0 = \boldsymbol{N}_v \cap \boldsymbol{N}_u$ of the two nullclines (see Fig.2(a)) is an equilibrium point since $(\dot{v},\dot{u}) = (0,0)$ at the point $(v,u) = \boldsymbol{S}_0$. In the case of Fig.2(a), any nearby point of the equilibrium point $\boldsymbol{S}_0$ is attracted into $\boldsymbol{S}_0$. From a neuron model viewpoint, such a phenomenon is called a *stable resting state* (ab. SRS) [9]. In the case of Fig.2(b), any nearby point of the equilibrium point $\boldsymbol{S}_0$ is repelled from $\boldsymbol{S}_0$. Such a phenomenon is called an *unstable resting state* (ab. URS).

Subthreshold oscillation. In the case of Fig.2(b), the state vector (v,u) continues to oscillate periodically under the spiking threshold V_T. From a neuron model viewpoint, such a phenomenon is called the periodic subthreshold oscillation [9]. If any nearby point is attracted into a periodic subthreshold oscillation, it is called a *stable periodic subthreshold oscillation* (ab. SSO). If any nearby point is repelled from a periodic subthreshold oscillation, it is called an *unstable periodic subthreshold oscillation* (ab. USO).

Tonic spiking. In the case of Fig.2(c), the state vector (v,u) continues to fire periodically. From a neuron model viewpoint, such a phenomenon is called a tonic spiking [9]. If any nearby point is attracted into a tonic spiking orbit, it is called a *stable tonic spiking* (ab. STS). If any nearby point is repelled from a tonic spiking orbit, it is called an *unstable tonic spiking* (ab. UTS).

In order to analyze these phenomena, we derive a return map as the followings. As shown in Fig.3(a), let an initial state of (v,u) on the u-nullcline $\boldsymbol{N}_u$ be denoted by (v_n,u_n). The point $(v_n,u_n) \in \boldsymbol{N}_u$ can be represented by its v-coordinate $v_n \in (-\infty, V_T]$. The trajectory starting from (v_n,u_n) returns into the u-nullcline $\boldsymbol{N}_u$ after visiting some of the vector fields $\{\boldsymbol{V}^{++},\boldsymbol{V}^{+-},\boldsymbol{V}^{-+},\boldsymbol{V}^{--},(0,0)\}$. As shown in Fig.3(a), let the return point of (v,u) on the u-nullcline $\boldsymbol{N}_u$ be denoted by (v_{n+1},u_{n+1}). Then the dynamics of the state v_n is described by the following one-dimensional return map F (see Fig.3(b)).

$$v_{n+1} = F(v_n), \quad F : (-\infty, V_T] \to (-\infty, V_T],$$

where $n = 1,2,3,\cdots$. For simplicity,

$$B = -V_T,\ I_v^+ = I_v^-,\ I_u^+ = I_u^-,\ I_u^+/I_v^+ = b,\ 1 < b < a \quad (3)$$

are assumed in this paper. Then the following analytic formula of the return map F can be derived.

$$v_{n+1} = F(v_n) = \begin{cases} \frac{a-b}{a+b} v_n & \text{if } E \le v_n < \frac{-(b-1)V_T}{a-b}, \\ \frac{2bV_{in}-(b+1)(a-b)v_n}{(b-1)(a+b)} & \text{if } \frac{(b-1)V_T}{a-b} \le v_n < V_{TR}, \\ \frac{2bV_{in}-(b-1)(a-b)v_n}{(b+1)(a+b)} & \text{if } V_{TR} \le v_n < V_T, \\ \frac{2bV_{in}-(b-1)(a+b)v_n}{(b+1)(a+b)} & \text{if } v_n = V_T, \end{cases} \quad (4)$$

where $V_{TR} \equiv V_{in}/(a-b)$. As shown in Figs.3(a) and 3(b), the value V_{TR} decides spiking or not, i.e., any trajectory starting from $(v_n,u_n) \in \boldsymbol{N}_u$ leads to a spiking if $v_n < V_{TS}$ and does not lead to a spiking if $V_{TS} \le v_n < V_T$. Hence we have the following proposition.

Proposition 1: Assume Equations (2) and (3) are satisfied. If the return map F has a fixed point $v_{rs} = F(v_{rs}) > V_{TR}$ and if the slope of the map satisfies $|dF(v_{rs})/dv_n| < 1$ ($|dF(v_{rs})/dv_n| > 1$), then the PWC analog spiking neuron model exhibits a stable resting state (unstable resting state). If the return map F has a periodic point $v_{so} = F^p(v_{so})$, $v_{so} \neq F^q(v_{so})$ for $1 \le q < p$ whose orbit points $(v_{so}, F(v_{so}), \cdots, F^{p-1}(v_{so}))$ are greater than V_{TR} and if the slope of the composed map satisfies $|dF^p(F(v_{so}))/dv_n| < 1$ ($|dF^p(F(v_{so}))/dv_n| > 1$), then the PWC analog spiking neuron model exhibits a stable periodic subthreshold oscillation (unstable periodic subthreshold oscillation). If the return map F has a fixed point $v_{ts} = F(v_{ts}) < V_{TR}$ and if the slope of the map satisfies $|dF(v_{ts})/dv_n| < 1$ ($|dF(v_{ts})/dv_n| > 1$), then the PWC analog spiking neuron model exhibits a stable tonic spiking (unstable tonic spiking).

We can confirm this proposition in Fig.4. In Fig.4(a), the return map has a stable fixed point $v_{rs} > V_{TR}$ and thus the PWC analog spiking neuron model exhibits a stable resting state. In Fig.4(b), the return map has stable periodic points $v_{so1} > V_{TR}$ and $v_{so2} > V_{TR}$, and thus the PWC analog spiking neuron model exhibits a stable subthreshold oscillation. In Fig.4(c), the return map has a stable fixed point $v_{ts} < V_{TR}$ and thus the PWC analog spiking neuron model exhibits a stable tonic spiking. In the following two subsections, we analyze bifurcation phenomena and related neural excitabilities of the PWC analog spiking neuron model.

A. *Supercritical Hopf type border-collision bifurcation*

In Fig.4(a), there exists a stable resting state. In Fig.4(b), the stimulation input V_{in} is increased. In this case the stable resting state is changed into an unstable resting state and the model exhibits a stable periodic subthreshold oscillation (see also Fig.5(a)). This change of phenomena (i.e., unstabilization of the resting state and birth of the stable periodic subthreshold oscillation) is caused by the discontinuous change of the slope of the return map F at the resting state v_{rs} that is referred to as the *border-collision bifurcation* [10]. In addition, the change of phenomena has qualitative similarities to the *supercritical Hopf bifurcation* [16]. Hence the change of phenomena between Figs.4(a) and 4(b) is referred to as a *supercritical Hopf type border-collision bifurcation*. In Fig.4(c), the input V_{in} is further increased. Then the stable periodic subthreshold oscillation is changed into a stable tonic spiking. This change of phenomena is caused by an effect of the spiking threshold V_T and is again referred to as the *border-collision bifurcation* [10]. As a result, the mechanisms (i.e., scenario) of the excitability from / to the stable resting state in Fig.4(a) to / from the tonic spiking in Fig.4(c) can be summarized as follows.

Excitability scenario A:

$$\begin{array}{c}\{\text{SRS}\}\\ \updownarrow\\ \{\text{URS, SSO}\}\\ \updownarrow\\ \{\text{URS, STS}\}\end{array}\qquad\begin{array}{l}\text{Supercritical Hopf type}\\ \text{border-collision bifurcation}\\ \\ \text{Border-collision bifurcation}\end{array}\qquad(5)$$

By using the return map F, we can derive the following sufficient parameter condition for the excitability scenario A.

The PWC analog spiking neuron model exhibits the excitability scenario A if $a > b^2$.

Fig.4(d) shows a bifurcation diagram for the stimulation input V_{in}, where the arrows α and β indicate the supercritical Hopf type border-collision bifurcation and the border-collision bifurcation, respectively. Fig.4(e) shows characteristics of the spiking frequency f defined by

$$f = \left(\frac{1}{M}\lim_{M\to\infty}\sum_{m=1}^{M}\Delta_m\right)^{-1}$$

where Δ_m is the m-th inter-spike interval in the output spike-train $Y(t)$ as shown in Fig.2(c). We emphasize that Izhikevich's simple neuron model exhibit a similar bifurcation scenario in Equation (5) and that the supercritical Hopf bifurcation is one of the typical mechanisms of excitabilities of biological and model neurons as explained in Table I.

B. *Fold limit cycle type border-collision bifurcation*

In Fig.6(c), the model exhibits co-existence of an stable resting state and a stable tonic spiking (see also Fig.5(b)). As the input V_{in} is decreased, the attraction domain of the stable resting state approaches to the stable tonic spiking. In the case of Fig.6(b), the attraction domain of the stable resting state touches the stable tonic spiking. If the input V_{in}

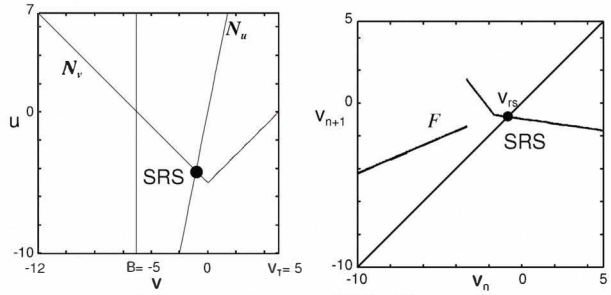

(a) *Stable resting state* (SRS). $V_{in} = -5$.

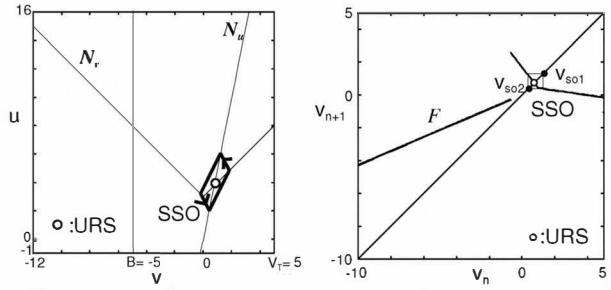

(b) Co-existence of *unstable resting state* (URS) and *stable periodic subthreshold oscillation* (SSO). $V_{in} = 3$.

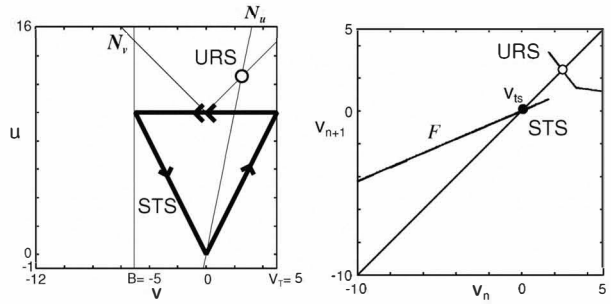

(c) Co-existence of *unstable resting state* (URS) and *stable tonic spiking* (STS). $V_{in} = 10$.

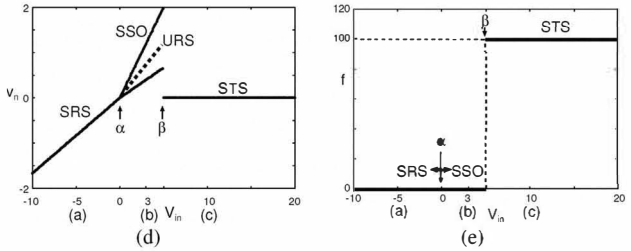

Fig. 4. Excitability scenario A in Equation (5). The parameters of the PWC analog spiking neuron model are $a = 5.0$, $I_v^+ = I_{\bar{v}} = 1.0$, $I_u^+ = I_{\bar{u}} = 2.0$, $V_T = 5.0$, $B = -V_T = -5.0$, and $C = 1.0 \times 10^{-3}$. (d) Bifurcation diagram. The arrows α and β indicate the supercritical Hopf type border-collision bifurcation and the border-collision bifurcation, respectively. (e) Characteristics of the spiking frequency f.

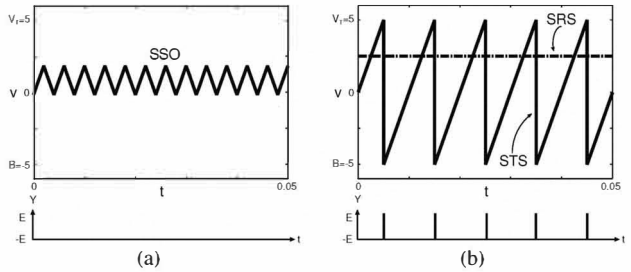

Fig. 5. Neuron-like time waveforms of v and Y. The parameter values in (a) and (b) are identical with those in Fig.4(b) and Fig.6(c), respectively.

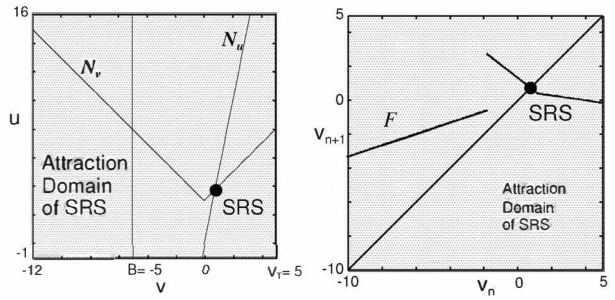

(a) *Stable resting state* (SRS). $V_{in} = 3$.

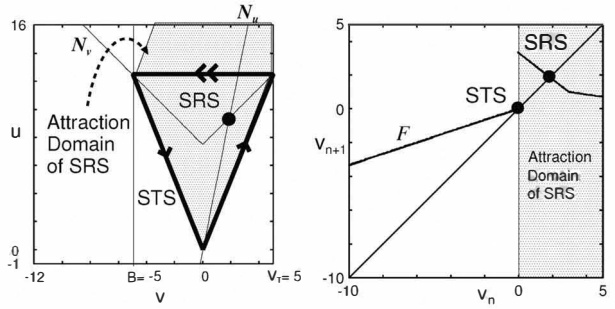

(b) Fold limit cycle type border-collision bifurcation. $V_{in} = 7.5$.

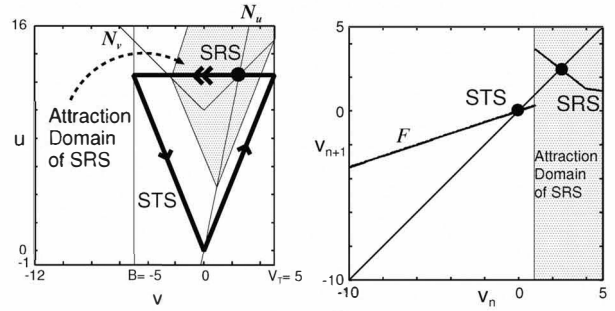

(c) Bistability. $V_{in} = 10$.

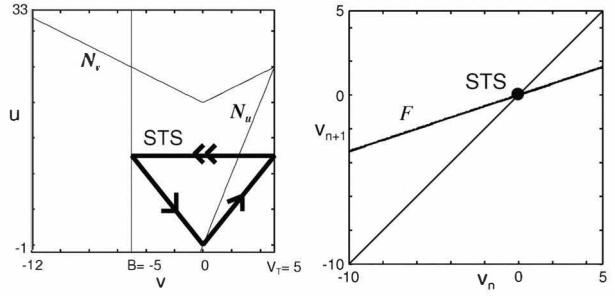

(d) *Stable tonic spiking* (STS). $V_{in} = 20$.

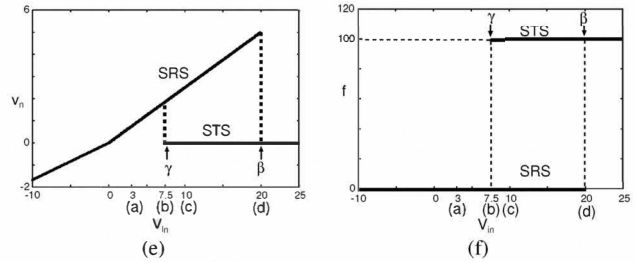

(e) (f)

Fig. 6. Excitability scenario B in Equation (6). The parameters of the PWC analog spiking neuron model are $a = 5.0$, $I_v^+ = I_v^- = 1.0$, $I_u^+ = I_u^- = 2.5$, $V_T = 5.0$, $B = -V_T = -5.0$, and $C = 1.0 \times 10^{-3}$. (e) Bifurcation diagram. The arrows γ and β indicate the fold limit cycle type border-collision bifurcation and the border-collision bifurcation, respectively. (f) Characteristics of the spiking frequency f.

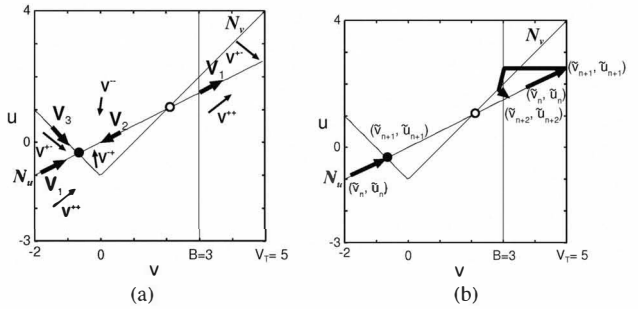

(a) (b)

Fig. 7. Sliding mode dynamics and return map G. (a) Sliding vector fields V_1, V_2, and V_3. (b) Phase-plane.

is further decreased, the stable tonic spiking is eaten by the attraction domain of the stable resting state and is vanished. This change of phenomena (i.e., vanish of the stable tonic spiking by the attraction domain of the stable resting state) is caused by the discontinuity of the return map F and has qualitative similarities to the *fold limit cycle bifurcation* [16]. Hence the change of phenomena between Figs.6(a) and 6(b) is referred to as a *fold limit cycle type border-collision bifurcation*. In Fig.6(d), the input V_{in} is increased compared to Fig.6(c). In this case the stable resting state is vanished due to the discontinuity of the return map F. As a result, the mechanisms (i.e., scenario) of the excitability from / to the stable resting state in Fig.6(a) to / from the tonic spiking in Fig.6(d) can be summarized as follows.

Excitability scenario B:

$$\begin{array}{c} \{\text{SRS}\} \\ \updownarrow \\ \{\text{SRS, STS}\} \\ \updownarrow \\ \{\text{STS}\} \end{array} \quad \begin{array}{l} \text{Fold limit cycle type} \\ \text{border-collision bifurcation} \\ \\ \text{Border-collision bifurcation} \end{array} \tag{6}$$

By using the return map F, we can derive the following sufficient parameter condition for the excitability scenario B.

The PWC analog spiking neuron model exhibits the excitability scenario B if $a < b^2$.

Fig.6(e) shows a bifurcation diagram for the stimulation input V_{in}, where the arrows γ and β indicate the fold limit cycle type border-collision bifurcation and the border-collision bifurcation, respectively. Fig.6(f) shows characteristics of the spiking frequency f. We emphasize that the the fold limit cycle bifurcation is often observed near a subcritical Hopf bifurcation which is one of the typical mechanisms of excitabilities of biological and model neurons as explained in Table I.

IV. Excitabilities with Sliding-mode

In this section we assume

$$0<a<1,\ a<\frac{I_u^+}{I_v^+},\ a<\frac{I_u^-}{I_v^-},\ 0<\frac{I_u^-}{I_v^+}<1,\ 1<\frac{I_u^+}{I_v^-}. \tag{7}$$

In this case, according to [10], the dynamics of the state vector (v, u) on the nullclines N_v and N_u can be described

by the following so-called sliding mode dynamics (see also Fig.7(a)).

$$(\dot{v},\dot{u}) = \begin{cases} \boldsymbol{V}_1 & \text{if } u=av \text{ and } \left(v<\frac{V_{in}}{a+1} \text{ or } -\frac{V_{in}}{1-a}<v<V_T\right), \\ \boldsymbol{V}_2 & \text{if } u=av \text{ and } \frac{V_{in}}{a+1}<v<-\frac{V_{in}}{1-a}, \\ \boldsymbol{V}_3 & \text{if } u=-v+V_{in} \text{ and } v<\frac{V_{in}}{a+1} \text{ and } v<0, \\ (0,0) & \text{if } u=av \text{ and } u=|v|+V_{in}, \end{cases} \tag{8}$$

where

$$\begin{aligned} \mathbf{V_1} &\equiv \frac{I_u^+-aI_v^+}{I_u^++I_u^-}\mathbf{V}^{+-}+\frac{I_u^-+aI_v^+}{I_u^++I_u^-}\mathbf{V}^{++}, \\ \mathbf{V_2} &\equiv \frac{I_u^--aI_v^-}{I_u^++I_u^-}\mathbf{V}^{-+}+\frac{I_u^++aI_v^-}{I_u^++I_u^-}\mathbf{V}^{--}, \\ \mathbf{V_3} &\equiv \frac{I_v^--I_u^-}{I_v^++I_v^-}\mathbf{V}^{+-}+\frac{I_v^++I_u^-}{I_v^++I_v^-}\mathbf{V}^{--}. \end{aligned} \tag{9}$$

In order to analyze the PWC analog spiking neuron model with the sliding mode, we derive another return map as the followings. As shown in Fig.7(b), let an initial state of (v,u) on the u-nullcline $\boldsymbol{N}_u$ be denoted by $(\tilde{v}_n,\tilde{u}_n)$, where "~" implies the sliding mode in this section. The point $(\tilde{v}_n,\tilde{u}_n)\in\boldsymbol{N}_u$ can be represented by its v-coordinate $\tilde{v}_n\in(-\infty,V_T]$. The trajectory starting from $(\tilde{v}_n,\tilde{u}_n)$ returns into the u-nullcline $\boldsymbol{N}_u$ after visiting some of the vector fields $\{\boldsymbol{V}^{++},\boldsymbol{V}^{+-},\boldsymbol{V}^{-+},\boldsymbol{V}^{--},(0,0),\boldsymbol{V}_1,\boldsymbol{V}_2,\boldsymbol{V}_3\}$ including the sliding mode vector fields $\boldsymbol{V}_1$, $\boldsymbol{V}_2$, and $\boldsymbol{V}_3$. As shown in Fig.7(b), let the return point of (v,u) on the u-nullcline $\boldsymbol{N}_u$ be denoted by $(\tilde{v}_{n+1},\tilde{u}_{n+1})$, where if a sliding mode trajectory reach a stable equilibrium point, then the stable equilibrium point is defined as the return point. Then the dynamics of the state $\tilde{v}_n$ is described by the following one-dimensional return map G (see Fig.8(b)).

$$\tilde{v}_{n+1}=G(\tilde{v}_n),\quad G:(-\infty,V_T]\to(-\infty,V_T],$$

where $n=1,2,3,\cdots$. For simplicity,

$$I_u^-/I_v^-=b,\ -I_u^-/I_v^+=c, c<0<a<1<b \tag{10}$$

are assumed in this paper. Then the following analytic formula of the return map G can be derived.

$$\tilde{v}_{n+1}=G(\tilde{v}_n)= \begin{cases} \frac{V_{in}}{a+1} & \text{if } v_n\le-\frac{V_{in}}{1-a} \text{ and } V_{in}\le 0, \\ V_T & \text{if } -\frac{V_{in}}{1-a}\le v_n<V_T, \\ V_T & \text{if } V_{in}>0 \text{ and } v_n<V_T, \\ V_R & \text{if } v_n=V_T, \end{cases} \tag{11}$$

where V_R is a constant defined by the parameters (a,B,V_T) and the input V_{in}. Depending on the value of V_R, the PWC analog spiking neuron model exhibits the following two types of excitability scenarios.

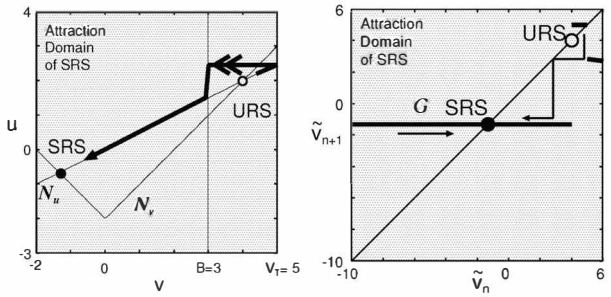

(a) *Stable Resting State* (SRS). $V_{in}=-2$.

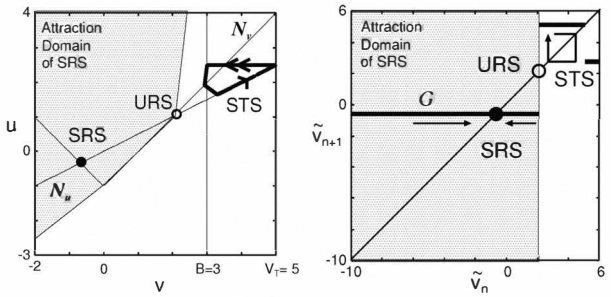

(b) Bistability. $V_{in}=-1$.

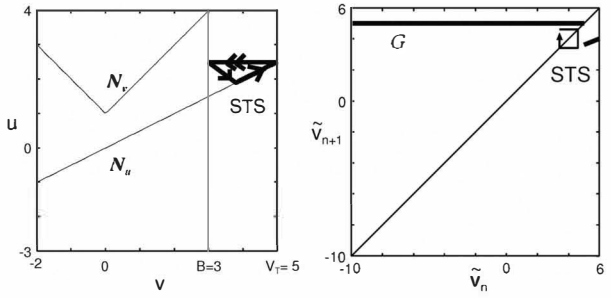

(c) *Stable Tonic Spiking* (STS). $V_{in}=1$.

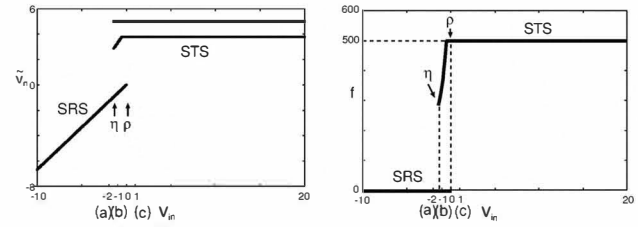

(d) (e)

Fig. 8. Excitability scenario C in Equation (13). The parameters of the PWC analog spiking neuron model are $a=0.5$, $I_v^+=1.0$, $I_v^-=0.1$, $I_u^+=I_u^-=0.75$, $V_T=5.0$, $B=3.0$, and $C=1.0\times10^{-3}$. (d) Bifurcation diagram. The arrows η and ρ indicate the saddle homoclinic type border-collision bifurcation and the saddle-node off invariant circle type border-collision bifurcation, respectively. (e) Characteristics of the spiking frequency f.

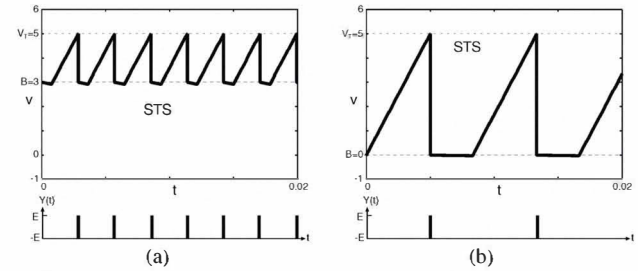

(a) (b)

Fig. 9. Neuron-like time waveforms of v and Y. The parameter values in (a) and (b) are identical with those in Fig.8(b) and Fig.10(b), respectively.

A. S-N off invariant circle type border-collision bifurcation

We assume $aV_T < B < V_T$. In this case the constant V_R of the return map G in Equation (11) is given by

$$V_R = \begin{cases} -\frac{bB-aV_T}{b-a} & \text{if } V_{in} \le (a-1)\frac{bB-aV_T}{b-a}, \\ \frac{(b-c)V_{in}+(1-c)(bB-aV_T)}{(a-c)(b-1)} & \text{if } (a-1)\frac{bB-aV_T}{b-a} < V_{in} < aV_T - B, \\ \frac{aV_T-cB}{a-c} & \text{if } aV_T - B \le V_{in}. \end{cases} \quad (12)$$

Fig.8 shows some return maps G and corresponding phase-plane trajectories. In Fig.8(b), the model exists co-existence of two stable phenomena: a stable resting state and a stable tonic spiking (see also Fig.9(a)). From a viewpoint of neuron model, this phenomena is called the bistability [9]. In Fig.8(a), the input V_{in} is decreased. In this case the stable tonic spiking is eaten by the attraction domain of the stable resting state. This change of phenomena (i.e., vanish of stable tonic spiking by the attraction domain of the stable resting state) is *the border-collision bifurcation* [10]. In addition, the change of phenomena has qualitative similarities to the *saddle homoclinic bifurcation* [16]. Hence the change of phenomena between Figs.8(a) and 8(b) is referred to as a *saddle homoclinic type border-collision bifurcation*. In Fig.8(c), the input V_{in} is increased compared to Fig.8(b). In this case the stable resting state vanishes since the intersection of the nullclines vanishes. Since the nullclines are the borders of vector fields, this change of phenomena is *the border-collision bifurcation* [10]. In addition, the change of phenomena (i.e., vanish of the stable resting state due to the vanish of the intersection of the nullclines) has qualitative similarities to the *saddle-node off invariant circle bifurcation* [16]. Hence the change of phenomena between Figs.8(b) and 8(c) is referred to as a *saddle-node off invariant circle type border-collision bifurcation*. As a result, the mechanisms (i.e., scenario) of the excitability from / to the stable resting state in Fig.8(a) to / from the tonic spiking in Fig.8(c) can be summarized as follows.

Excitability scenario C:

$$\begin{array}{ll} \{\text{SRS, URS}\} & \text{Saddle homoclinic type} \\ \updownarrow & \text{border-collision bifurcation} \\ \{\text{SRS, URS, STS}\} & \\ \updownarrow & \text{Saddle-node off invariant circle} \\ \{\text{STS}\} & \text{type border-collision bifurcation} \end{array} \quad (13)$$

Fig.8(d) shows a bifurcation diagram for the stimulation input V_{in}, where the arrows η and ρ indicate the saddle homoclinic type border-collision bifurcation and the saddle-node off invariant circle type border-collision bifurcation, respectively. Fig.8(e) shows characteristics of the spiking frequency f. We emphasize that Izhikevich's simple neuron model exhibit a similar bifurcation scenario in Equation (13) and that the saddle-node off invariant circle bifurcation is one of the typical mechanisms of excitabilities of biological and model neurons as explained in Table I.

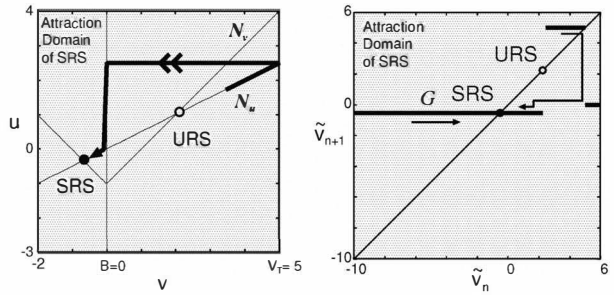

(a) *Stable Resting State* (SRS). $V_{in} = -1$.

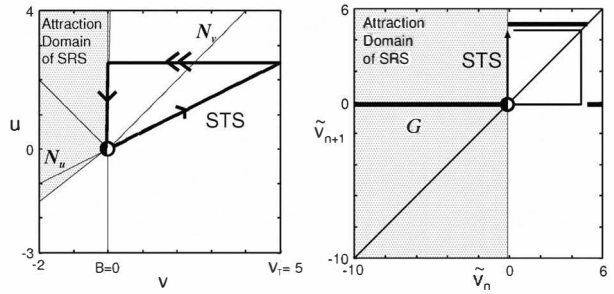

(b) Saddle-node on invariant circle type Border-collision bifurcation. $V_{in} = 0$.

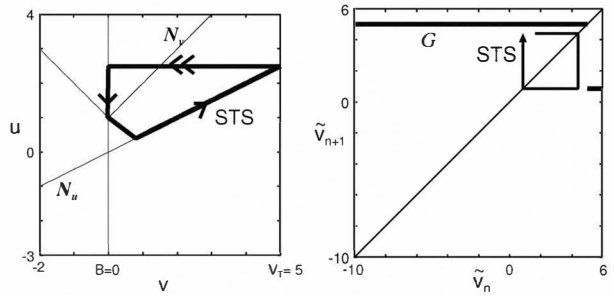

(c) *Stable Tonic Spiking* (STS) with low firing frequency. $V_{in} = 1$.

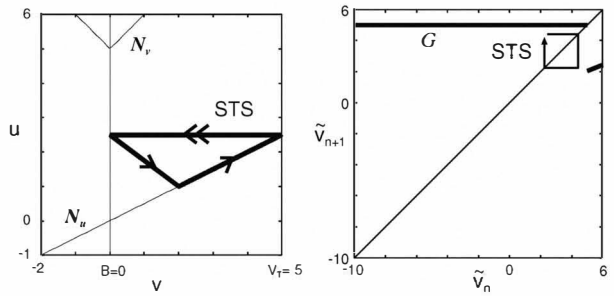

(d) *Stable Tonic Spiking* (STS) with high firing frequency. $V_{in} = 5$.

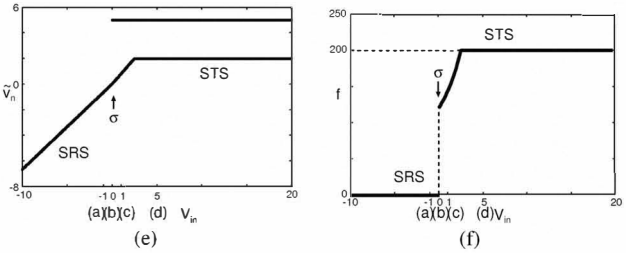

Fig. 10. Excitability scenario D in Equation (15). The parameters of the PWC analog spiking neuron model are $a = 0.5$, $I_v^+ = 1.0$, $I_v^- = 0.01$, $I_u^+ = I_u^- = 0.75$, $V_T = 5.0$, $B = 0.0$, and $C = 1.0 \times 10^{-3}$. (e) Bifurcation diagram. The arrow σ indicates the saddle-node on invariant circle type border-collision bifurcation. (f) Characteristics of the spiking frequency f.

B. S-N on invariant circle type border-collision bifurcation

Here we assume $B = 0$. In this case the constant V_R of the return map G in Equation (11) is given by

$$V_R = \begin{cases} -\frac{a}{b-a}V_T & \text{if} \quad V_{in} < 0, \\ \frac{V_{in}}{a-c} & \text{if} \quad 0 \leq V_{in} < aV_T, \\ \frac{aV_T}{a-c} & \text{if} \quad V_{in} \geq aV_T. \end{cases} \tag{14}$$

In Fig.10(c), there exists a stable tonic spiking. As the input V_{in} is decreased, as shown in Fig.10(b), the stable tonic spiking includes a point at which the minimum of the v-nullcline $\boldsymbol{N}_v$ touches the u-nullcline $\boldsymbol{N}_v$ (see also Fig.9(b)). As the input V_{in} is further decreased, as shown in Fig.10(a), the stable tonic spiking is eaten by the attraction domain of the stable resting state and then the stable tonic spiking is vanished. This change of phenomena is caused by the discontinuity of the return map G and thus it is the *border-collision bifurcation* [10]. In addition, the change of phenomena has qualitative similarities to the *saddle-node on invariant circle bifurcation* [16]. Hence the change of phenomena among Figs.10(a), 10(b), and 10(c) is referred to as a *saddle-node on invariant circle type border-collision bifurcation*. This mechanism (i.e., scenario) of the excitability from / to the stable resting state in Fig.10(a) to / from the tonic spiking in Fig.10(d) can be summarized as follows.

Excitability scenario D:

$$\begin{array}{c} \{\text{SRS, URS}\} \\ \updownarrow \\ \{\text{STS}\} \end{array} \quad \text{Saddle-node on invariant circle type border-collision bifurcation} \tag{15}$$

In Fig.10(d), the input V_{in} is increased compared to Fig.10(c). In this case the model exhibits a stable tonic spiking with a higher spiking frequency f. Fig.10(e) shows a bifurcation diagram for the stimulation input V_{in}, where the arrow σ indicates the saddle-node on invariant circle type border-collision bifurcation. Fig.10(f) shows characteristics of the spiking frequency f. We emphasize that Izhikevich's simple neuron model exhibit a similar bifurcation scenario in Equation (15) and that the saddle-node on invariant circle bifurcation is one of the typical mechanisms of excitabilities of biological and model neurons as explained in Table I.

V. Bursting with Sliding-mode

We assume $1 < a$, $I_u^+/I_v^+ < 1$, $I_u^-/I_v^+ < 1$, and $B > 0$. In this case, the PWC spiking neuron may exhibit *tonic bursting* [9] as shown in Fig.11. According to [9], the tonic bursting is one of the most fundamental neurocomputational properties of biological neurons. The bifurcation analysis of the tonic bursting is omitted in this paper due to the page length limitation and will be presented in a future paper.

VI. Discussions and Conclusions

We have proposed the novel *piece-wise constant* (ab. PWC) analog spiking neuron model. Using the analytical return maps, it has been shown that the model can reproduce the typical relations among neural behaviors and their underlying bifurcations as explained in Table I. Future problems include: (a) implementation of this model in an actual hardware, (b) reproduction of a *subcritical Hopf type bifurcation* which leads to a monostability and a subthreshold oscillation, and (c) more in-depth theoretical analysis of excitability and bifurcations.

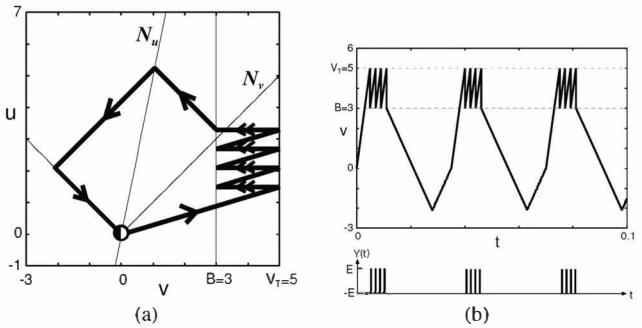

Fig. 11. Tonic bursting. The parameters of the PWC analog spiking neuron model are $a = 5.0$, $I_v^+ = 1.0$, $I_v^- = I_u^+ = I_u^- = 0.3$, $V_T = 5.0$, $B = 3.0$, $C = 1.0 \times 10^{-3}$, and $V_{in} = 0$. (a) Phase Plane. (b) Time waveforms of v and Y.

The authors would like to thank Professor Toshimitsu Ushio of Osaka University for valuable discussions. This work is partially supported by KAKENHI (21700253).

References

[1] E. Izhikevich, "Simple model of spiking neurons," *IEEE Trans. Neural Netw.*, vol. 14, no. 6, pp. 1569–1572, 2004.
[2] G. Indiveri, E. Chicca, and R. Douglas, "A VLSI Array of Low-Power Spiking Neurons and Bistable Synapses With Spike-Timing Dependent Plasticity," *IEEE Trans. Neural Netw.*, vol. 17, no. 1, p. 211, 2006.
[3] T. Yu and G. Cauwenberghs, "Analog VLSI Biophysical Neurons and Synapses With Programmable Membrane Channel Kinetics," *IEEE Trans. Biomed. Circuits Syst.*, vol. 4, no. 3, pp. 139–148, 2010.
[4] T. Asai, Y. Kanazawa, and Y. Amemiya, "A subthreshold MOS neuron circuit based on the Volterra system," *IEEE Trans. Neural Netw.*, vol. 14, no. 5, pp. 1308–1312, 2003.
[5] E. Farquhar and P. Hasler, "A bio-physically inspired silicon neuron," *Regular Papers, IEEE Trans. CAS-I*, vol. 52, no. 3, pp. 477–488, 2005.
[6] A. Basu and P. Hasler, "Nullcline-Based Design of a Silicon Neuron," *Regular Papers, IEEE Trans. CAS-I*, no. 99, p. 1.
[7] M. Simoni and S. DeWeerth, "Adaptation in a VLSI model of a neuron," *Analog and Digital Signal Processing, IEEE Trans. CAS-II*, vol. 46, no. 7, pp. 967–970, 2002.
[8] T. Kohno and K. Aihara, "A MOSFET-based model of a class 2 nerve membrane," *IEEE Trans. Neural Netw.*, vol. 16, no. 3, pp. 754–773, 2005.
[9] E. Izhikevich, *Dynamical systems in neuroscience: The geometry of excitability and bursting.* The MIT press, 2007.
[10] M. Di Bernardo, *Piecewise-smooth dynamical systems: theory and applications.* Springer Verlag, 2008.
[11] Berger *et al.*, "Restoring lost cognitive function." *IEEE Eng. Med. Biol. Mag.*, vol. 24, no. 5, p. 30.
[12] T. Berger and D. Glanzman, *Toward replacement parts for the brain: implantable biomimetic electronics as neural prostheses.* The MIT Press, 2005.
[13] Y. Matsuoka, T. Hasegawa, and T. Saito, "Chaotic Spike-Train with Line-Like Spectrum," *IEICE Trans. Fund.*, vol. E92-A, no. 4, pp. 1142–1147, 2009.
[14] Y. Matsuoka and T. Saito, "A Simple Chaotic Spiking Oscillator Having Piecewise Constant Characteristics," *IEICE Trans. Fund.*, vol. E89-A, no. 9, pp. 2437–2440, 2006.
[15] T. Tsubone and T. Saito, "Manifold Piecewise Constant Systems and Chaos," *IEICE Trans. Fund.*, vol. E82-A, no. 8, pp. 1619–1626, 1999.
[16] Y. Kuznetsov, I. Kuznetsov, and Y. Kuznetsov, *Elements of applied bifurcation theory.* Springer New York, 1998.